

Noninvasive characterization of renal artery blood flow

ERNEST R. GREENE, MICHAEL D. VENTERS, PRATAP S. AVASTHI, RICHARD L. CONN, and
ROBERT W. JAHNKE

*Clinical Research Division, Lovelace Medical Foundation, and Department of Nephrology, Veterans Administrative Medical Center
University of New Mexico School of Medicine, Albuquerque, New Mexico*

Noninvasive characterization of renal artery blood flow. Noninvasive characterization of renal artery blood flow variables in the human has not been reported. Using a unique dual-frequency real-time two-dimensional echo Doppler (Duplex scanner) that was calibrated in vitro, we characterized renal artery blood flow patterns in 16 normal subjects (6 females). Calculated mean values of systolic diameter (D_s), maximal spatial average blood velocity (V_{msa}), and volume flow rate (\dot{Q}) were as follows: 4.5 ± 0.6 mm right, 4.4 ± 0.6 mm left; 67.6 ± 9.4 cm \cdot sec $^{-1}$ right, 69.6 ± 12.0 cm \cdot sec $^{-1}$ left; and 403 ± 127 ml \cdot min $^{-1}$ right, 395 ± 98 ml \cdot min $^{-1}$ left; respectively. Direct linear regression correlation of body surface area (BSA) with D_s and \dot{Q} were statistically significant ($P < 0.01$, $r = 0.70$; and $P < 0.01$, $r = 0.72$, respectively). In a blind prospective series, six of seven angiographically normal renal arteries were noninvasively identified by normal geometry and blood velocity patterns. One angiographically normal artery was incorrectly classified as mildly stenotic. Eleven angiographically documented abnormal renal arteries were noninvasively identified by their abnormal blood flow patterns and/or geometry. This study suggests that dual-frequency Duplex scanning with careful sample volume control and Doppler audio spectra/blood velocity waveform analysis can be used to characterize blood flow variables in normal and diseased human renal arteries.

Etude non invasive du débit sanguin dans l'artère rénale. L'étude non invasive des variables du débit sanguin dans l'artère rénale chez l'homme n'a pas été rapportée. Nous avons utilisé un écho Doppler original bi-dimensionnel en temps réel à double fréquence (Duplex scanner) calibré in vitro pour établir les modalités du débit sanguin artériel rénal chez seize sujets normaux dont six de sexe féminin. Les valeurs moyennes calculées du diamètre systolique (D_s), de la vitesse sanguine spatiale maximale moyenne (V_{msa}), et du débit (\dot{Q}) étaient respectivement les suivantes: $4,5 \pm 0,6$ mm à droite, $4,4 \pm 0,6$ mm à gauche; $67,6 \pm 9,4$ cm \cdot sec $^{-1}$ à droite, $69,6 \pm 12,0$ cm \cdot sec $^{-1}$ à gauche; et 403 ± 127 ml \cdot min $^{-1}$ à droite, 395 ± 98 ml \cdot min $^{-1}$ à gauche. Les régressions linéaires par rapport à la surface corporelle étaient significatives pour D_s et \dot{Q} ($P < 0,01$, $r = 0,70$; et $P < 0,01$, $r = 0,72$; respectivement). Dans une série prospective aveugle six parmi sept artères rénales normales à l'angiographie ont été identifiées de façon non invasive par la géométrie et les modalités de vitesse sanguine normales. Une artère normale à l'angiographie a été classée comme moyennement sténotique. Onze artères anormales à l'angiographie ont été identifiées de façon non invasive par leurs modalités de débit sanguin et/ou leur géométrie anormales. Ces résultats suggèrent que l'appareil peut être utilisé pour déterminer les variables du débit sanguin dans les artères normales et lésées chez l'homme.

Standard methods of diagnosing renal artery abnormalities are either undefinitive [1] or invasive [2, 3]. Although various forms of renal pathology can be demonstrated using abdominal gray-scale ultrasonography [4], renal artery stenosis due to congenital bands, fibromuscular hyperplasia, or atheroma cannot be reliably detected noninvasively. Recent advances in

pulsed ultrasound Doppler techniques have provided a quantitative assessment of blood-flow characteristics in both normal and diseased blood vessels [5]. Clinical application of these methods in detecting arterial lesions have been successfully applied to cardiac [6, 7] and peripheral vascular disease [8, 9]. Noninvasive pulsed Doppler flowmetry has not previously been applied to the human renal artery. The purpose of this study was to evaluate the feasibility of measuring blood flow variables in both normal and diseased human renal arteries.

Methods

Instrumentation. We used a unique, dual-frequency (3 and 5 mHz) Duplex scanner (DS) (Mark V Model, Advanced Technology Laboratories, Bellevue, Washington) whose theoretical and technical characterization has been previously described in detail [5-8]. Basically, the device incorporates a real-time, two-dimensional 90° sector image duplexed with a range-gated pulsed Doppler. The duplex method is based upon the ability of the system to define the walls along the longitudinal axis of an imaged vessel. Simultaneously, the detected pulsed Doppler ultrasound audio spectra are used to evaluate the changes in the blood velocities within the artery visualized. The imaging and Doppler systems are operated at either 3.0 or 5.0 mHz and are connected to a single scanhead. The choice of frequency depends on the penetration requirements specific for each subject. Generally, the 5.0-mHz frequency provides adequate penetration with maximum resolution for an optimal sector scan. The Doppler beam axis can be moved to any location in the sector scan. The variable sample volume [5] can be placed at any given point 3 to 17 cm along the Doppler beam. The real-time image, which includes the Doppler beam axis and the location of the range-gated sample volume, was displayed on a video monitor. The combined M-mode and Doppler signals [6] were also displayed on a second video monitor. All images, Doppler audio (time-interval histogram) and analog (zero-crosser) signals, EKG lead II, and a control voice track were recorded on a video tape recorder (HP 2800) with forward and reverse audio channels. A foot-switch control allowed any of

Received for publication January 12, 1981
and in revised form March 12, 1981

0085-2538/81/0020-0523 \$01.40

© 1981 by the International Society of Nephrology

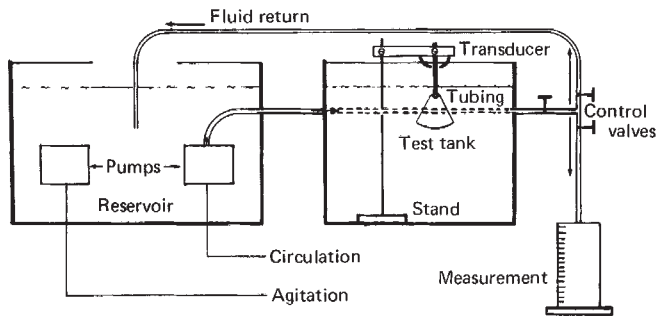


Fig. 1. Schematic representation of the flow tank used in the *in vitro* calibrations. Note the axis of the Doppler beam depicted on the two-dimensional scan plane. From the video image of the scan plane, Doppler angles and vessel internal diameter can be measured with a protractor and caliper. θ is Doppler angle; V_{sa} , spatial average velocity; I.D., internal diameter.

the displayed signals to be recorded on a fiberoptic recording system. Because the linearity of the time-interval histogram (TIH) and analog (zero-crosser-blood velocity) signals depends on the width of the Doppler audio spectra [5], an off-line fast Fourier spectrum analyzer (Nicolet 446) was also used throughout all the measurement periods to display selected Doppler audio spectra and to calibrate the Doppler TIH and analog signals [10]. The calibrated analog signal was subsequently used in calculation of blood flow variables with the TIH providing a real-time estimation of the spectrum width and hence the accuracy of the analog waveform.

Measured variables. From the carefully controlled sample volume [12, 13], a minimum of five analog audio spectrum waveforms (Δf) representing the spatially averaged blood velocity within the imaged lumen were recorded. Using the unique EKG triggered freeze-frame capability of the DS, longitudinal two-dimensional images of the vessel were obtained at desired points in the cardiac cycle. We used calipers to measure the peak systolic vessel diameter (D_s) (± 0.2 mm) from the gray scale, video display, and the hard-copy images. With a protractor, Doppler incident angles ($\pm 1^\circ$) to the flow direction (θ) were also measured. The flow direction is assumed to be streamlined and parallel to the imaged vessel walls. Due to the critical nature of the measurements of D_s and θ [5], two investigators made independent determinations from the video and hard-copy images, and the average values of D_s and θ were used in subsequent calculation of blood velocity variables. It should be noted that there exists a well-recognized deterioration of the image quality and resolution when the video image is transformed into hard copy visicorder printouts and published photographs. Full appreciation of the image quality and hence measured dimensions and angles can only be made during the real-time demonstration on the video monitors.

Calculated variables. Using the average values of D_s , θ , and five digitized cycles of Δf , a microcomputer system (Intel 3000) calculated, averaged (\pm SD), and printed the following variables: (1) the heart rate (HR); (2) the spatial average velocity (V_{sa}) using the Doppler equation:

$$V_{sa} = \frac{\Delta f \cdot C}{2 \cdot f \cdot \cos \theta} \text{ (cm} \cdot \text{sec}^{-1}\text{)}$$

where Δf is the audio spectrum analog waveform (Hz) repre-

senting the spatially averaged blood velocity, C is the velocity of sound in blood (1.5×10^5 cm \cdot sec $^{-1}$), f is the transmitted frequency (3 or 5 mHz), and θ is the Doppler angle (measured from the vessel image); (3) the maximum spatial average velocity in the cardiac cycle (V_{msa}); (4) the temporal mean of spatial average velocity in the cardiac cycle (\bar{V}_{sa}), where $\bar{V}_{sa} = \int V_{sa} dt / \int dt$ (cm \cdot sec $^{-1}$); and (5) the volume flow rate (\dot{Q}) using the equation $\dot{Q} = \pi D_s^2 \cdot \bar{V}_{sa} / 4$ (ml \cdot min $^{-1}$).

In vitro calibration. The *in vitro* calibration was conducted in a specially designed flow system [12] (Fig. 1). In a flexible tube (4.00 mm I.D., 4.5 mm O.D.), cellular particles were suspended in distilled water to simulate the scattering properties of erythrocytes. At selected Reynolds numbers [14], Doppler audio TIH and analog recordings of the spatial average velocity were obtained. The Reynolds numbers and flow rates were carefully controlled to simulate hemodynamic conditions in the human renal artery. Doppler angles, θ , were used which were consistent to those used in the subsequent *in vivo* studies (50° to 80°). The values of the measured and calculated flow variables determined by the DS method were compared with values obtained from flow collection data and direct caliper measurements of the lumen diameter.

Subject population. A control group of 16 volunteer subjects (6 females) ranging in age from 15 to 53 years (mean, 28 ± 8 years) and body surface area (BSA) from 1.34 to 2.08 m 2 (mean, 1.75 ± 0.18 m 2) were included in the study. This control group was taken from 21 consecutive volunteers, of which five studies (24%) were technically unsatisfactory due to inadequate imaging and/or blood velocimetry. All volunteer subjects had a normal renal function as documented by the standard renal function tests. To determine the reproducibility of the method, we studied one individual on 3 separate days under identical circumstances. Prior to their participation in the study, the subjects signed consent forms, which were approved by the Human Subjects Review Committee.

In a subsequent blind study of 11 consecutive patients, 2 (18%) had technically inadequate studies. The remaining 9 patients (4 female) with clinically suspected renal artery abnormalities were studied noninvasively and angiographically. Measured and calculated blood flow variables from these patients were compared with values obtained in the control group. In the case of unilateral disease, flow variables from one renal vessel were compared with the normal contralateral vessel. Results of the noninvasive and angiographic studies were compared.

In vivo measurement procedure. The 16 normal subjects and the 9 patients were studied after they had fasted. This condition insured minimal signal interference from stomach and bowel gas. If abdominal gas was present, the procedure was undertaken at a later time. Subjects were placed in the supine position with lead II EKG attached. The optimal acoustic window was generally obtained 2 to 3 cm caudal to the xyphoid process of the rib cage along the centerline of the abdomen [4]. Initially, the long axis of the abdominal aorta was displayed with a parallel segment of the superior mesenteric artery viewed anteriorly. Using these anatomical features as landmarks, the scanhead was rotated 90° and moved cranially and caudally in the frontal plane until a cross-section of the abdominal aorta and a long axis view of one or both of the renal arteries were imaged. Often the renal arteries originated in different transverse planes. After the renal arteries and landmarks were

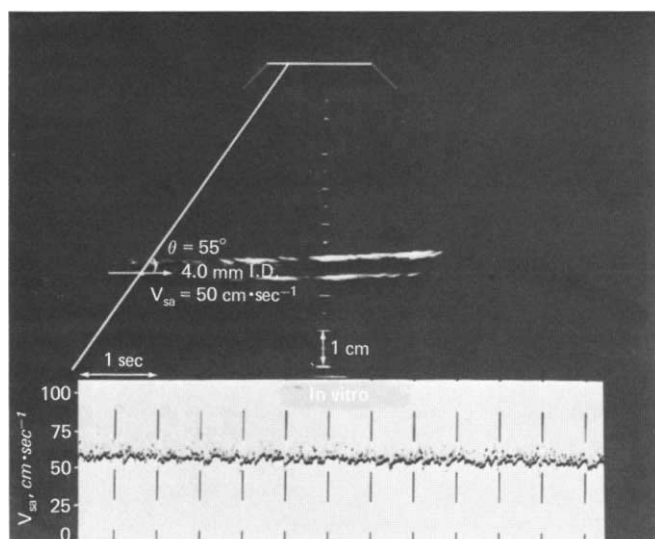


Fig. 2. Representative gray-scale image and spatial average velocity (V_{sa}) waveform obtained during in vitro flow tank simulation. The Doppler angle was arbitrarily set at values of 50° to 80° . Other abbreviations are θ , Doppler angle; V_{sa} , spatial average velocity, I.D., internal diameter.

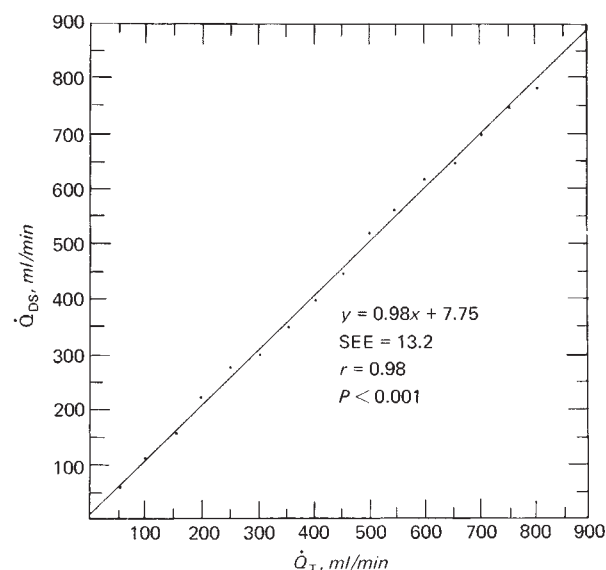


Fig. 3. Regression curve relating direct flow measurements (Q_T) and calculated flow from the Duplex scanner (Q_{DS}) obtained during flow tank simulation.

identified, the gain and reject settings of the imager were set to accentuate the near and far walls of the renal arteries. This maneuver often obscured the proximal anatomical features, but provided the most accurate means of estimating the renal artery diameter. Often the renal arteries were traced laterally to their bifurcation near the renal pelvis. With the renal artery visualized, the sample volume was manually placed in the vessel and varied in axial dimension appropriately to allow uniform insonification of the velocity profile from the anterior and posterior imaged renal walls [5, 12]. The Doppler audio signals, systolic diameter, and Doppler angle with the flow streamline (assumed parallel to vessel walls) were then recorded. It is most important to note that the added Doppler capability with variable sample volume control of the DS facilitates distinction between vascular and nonvascular structures and between arterial and venous signals. Consequently, the various vascular features in the abdominal cavity such as the lumen of the renal artery can be delineated from the anteriorly positioned renal vein. In addition, the low impedance of the renal vascular system creates a relatively high diastolic blood flow characteristic that is not present in the abdominal aorta. To minimize respiration artifacts, all recordings were made during breath holding at midexpiration. Because great care was required to obtain optimal images and signals, the procedure generally required between 30 min to 1 hour of the subject's time.

Statistical analysis. Standard linear regression analysis and product moment correlations were used in the following comparisons: (1) controlled with calculated blood flow variables obtained during the in vitro calibration and (2) various in vivo blood flow variables with body surface areas (BSA). Student's paired t tests were used in comparing left and right blood flow variables. Due to the limited number of angiographic correlates available in this preliminary study, only a descriptive comparison between DS and angiographic results can be given.

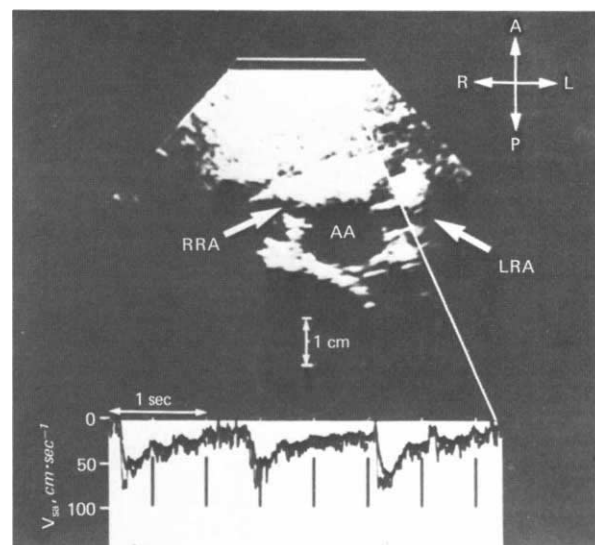


Fig. 4. Representative transverse gray-scale image and spatial average velocity (V_{sa}) waveform from the left renal artery (LRA) obtained noninvasively from a normal subject. Instrument settings are adjusted to accentuate the renal artery walls. Other abbreviations are AA, abdominal aorta; RRA, right renal artery.

Results

In vitro calibration. Figure 2 illustrates a longitudinal image of the 4.0-mm I.D. tubing in the in vitro calibration system. Note that the Doppler beam axis and angle to the flow streamline are not assumed but are measured. Superimposed on the image are the TIH (dot pattern) and the calibrated velocity analog signal V_{sa} . In this case, the spatial average velocity was controlled at $50.0 \text{ cm} \cdot \text{sec}^{-1}$ and measured with the DS as $52.8 \text{ cm} \cdot \text{sec}^{-1}$. The minimal spreading of the TIH signal dictates a

Table 1. Measured and calculated variables of right (R) and left (L) renal artery blood flow in 16 normal subject population^a

| Age years | BSA m^2 | D_s mm | θ degrees | V_{msa} $cm \cdot sec^{-1}$ | \bar{V}_{sa} $cm \cdot sec^{-1}$ | \dot{Q} $ml \cdot min^{-1}$ |
|--------------|-------------|-------------|---------------------|----------------------------------|---------------------------------------|----------------------------------|
| 28 ± 8 | 1.75 ± 0.18 | R 4.5 ± 0.6 | 71 ± 7 | 67.6 ± 9.4 | 40.9 ± 8.1 | 403 ± 127 |
| | | L 4.4 ± 0.6 | 73 ± 6 | 69.7 ± 12.1 | 41.0 ± 7.6 | 396 ± 98 |

^a Abbreviations are defined as BSA, body surface area; D_s , systolic diameter; θ , Doppler angle; V_{msa} , maximum spatial average velocity; \bar{V}_{sa} , temporal mean of the spatial average velocity; \dot{Q} , volume flow rate. Values are the means ± SD.

Table 2. Linear regressions (LR), correlation coefficients, and levels of significance for comparisons of body surface area (BSA) and systolic diameter (D_s) and volume flow rate (\dot{Q}) from 16 normal subjects

| | | | LR | <i>r</i> | <i>P</i> |
|---|--------------|------------|----------------------|----------|----------|
| BSA (<i>x</i>) vs. <i>D_s</i> (<i>y</i>) | Left | <i>y</i> = | 0.06 + 2.51 <i>x</i> | 0.74 | <0.01 |
| | Right | <i>y</i> = | 0.36 + 2.37 <i>x</i> | 0.71 | <0.01 |
| | Left + right | <i>y</i> = | 0.21 + 2.44 <i>x</i> | 0.72 | <0.01 |
| BSA (<i>x</i>) vs. <i>Q̇</i> | Left | <i>y</i> = | -263 + 376 <i>x</i> | 0.70 | <0.01 |
| | Right | <i>y</i> = | -472 + 500 <i>x</i> | 0.71 | <0.01 |
| | Left + right | <i>y</i> = | -367 + 438 <i>x</i> | 0.70 | <0.01 |

narrow Doppler audio spectrum and is used to qualitatively assess the distribution of blood velocities in the sample volume and hence the linearity and accuracy of the analog signal V_{sa} [10]. In this simple form of spectral analysis (TIH), a wider dot pattern would suggest a broader Doppler audio spectra due to transient or steady-state flow disturbances. Consequently, the accuracy of the analog signal V_{sa} would be compromised. Here the bandwidth of the Doppler audio spectra is sufficiently small (as indicated by the TIH and verified by the fast Fourier analysis) to accept the analog signal V_{sa} . Figure 3 illustrates the regression curve which relates \dot{Q} calculated from the DS measurement (\dot{Q}_{DS}) and from direct measurement in the tank (\dot{Q}_T). Under this condition of minimal experimental error, there was a strong correlation ($r = 0.98$) between \dot{Q}_{DS} and \dot{Q}_T . The slope of the regression was near unity (0.98) with a relatively small y intercept (7.75) and standard error of the estimate (13.2). Even at the higher values of θ , \dot{Q}_{DS} varied only ± 5%. The correlation of \dot{Q}_{DS} and \dot{Q}_T was independent of θ [5].

In vivo measurements. Figure 4 illustrates both the left (LRA) and right (RRA) renal arteries at their origin from the abdominal aorta (AA) in a normal subject. Here the instrument settings are adjusted to obscure the proximal anatomy and delineate the renal arteries. A typical calibrated analog V_{sa} waveform from the left renal artery is presented in the lower portion of Fig. 4. Note the TIH signal demonstrates a minimal dot pattern, suggesting a laminar, accelerating velocity profile [5, 14]. Blood velocities toward and away from the plane of the Doppler beam axis are recorded above and below the baseline. Normal renal V_{sa} is characterized by a rapid forward phase during systole with continuous diastolic flow. From the video image of the LRA, the interoperator averaged D_s was measured as 4.5 mm with θ measured as 72°. Blood flow variables in this normal subject were averaged as $V_{msa} = 58.4 \pm 7.5 \text{ cm} \cdot \text{sec}^{-1}$; $\bar{V}_{sa} = 35.1 \pm 4.5 \text{ cm} \cdot \text{sec}^{-1}$; and $\dot{Q} = 335 \pm 44 \text{ ml} \cdot \text{min}^{-1}$.

Table 1 represents a summary of the mean data derived from the 16 normal subjects. The average values of V_{msa} were 67.6 ± 9.4 and $67.7 \pm 12.1 \text{ cm} \cdot \text{sec}^{-1}$ for the right and left renal arteries, respectively. The average values of D_s were 4.5 ± 0.6 right and 4.4 ± 0.6 mm left. The average values of \dot{Q} were 403 ± 127 right and $396 \pm 98 \text{ ml} \cdot \text{min}^{-1}$ left. There was no statistically significant difference between averaged right and left values of any of the measured or calculated variables.

Table 2 presents the correlation coefficients, linear regression equations, and levels of significance derived from the comparisons of BSA and blood flow variables (D_s and \dot{Q}). Statistically significant ($P < .01$) direct correlations were found between D_s and \dot{Q} and BSA. There were no significant correlations ($P < 0.10$) between V_{msa} or \bar{V}_{sa} and BSA.

As an indicator of the reproducibility of the method, Table 3 contains data obtained on three separate occasions from the same individual by the same investigator (ERG) over a period of 3 weeks. Although there is some variability between the measured and calculated variables, it is well within a physiologically acceptable range, and the standard deviations are relatively small. One should note that the value of θ depends on the transducer/vessel configuration and is set arbitrarily to a minimal value consistent with image quality. Again, different values of θ did not appear to greatly affect the calculated variables.

Angiographic correlates. In the blind study of 9 patients (18 renal arteries) who underwent renal artery angiography, results from the noninvasive study were graded as follows:

Grade 1: Normal. Bilateral values of D_s and \dot{Q} within 1 SD of the normalized mean values (D_s/BSA ; \dot{Q}/BSA) obtained from the control group.

Grade 2: Proximal partial obstruction. A focal lesion at the origin of the renal artery demonstrated by reduced lumen cross-section or measured convective increases in V_{sa} , or increased Doppler audio spectra broadening within the vessel cross-section [7–10]. Values of D_s/BSA below and/or values of V_{msa}/BSA above 1 SD of the normalized mean value with audio spectra broadening were obtained from the control group.

Grade 3: Increased vascular impedance. Values of \dot{Q} below one standard deviation of the normalized mean value obtained from the contralateral vessel or the control group. The reduced values of V_{sa} and \dot{Q} reflect an increase in distal arterial impedance due to a hemodynamically significant distal stenosis, microvascular disease, and/or reduced vascularity as subsequently indicated by angiography, renal vein renins, radiographic renal size, and nuclear imaging.

Grade 4: Proximal occlusion. No lumen image or blood velocities recorded.

Figure 5 illustrates the RRA and LRA angiographic (upper portion) findings and the gray-scale image and velocity waveforms (lower portion) from a 33-year-old female hypertensive patient. The V_{sa} waveform of the RRA exhibits significantly reduced diastolic flow velocity when compared to the LRA,

Table 3. Measured and calculated variables for renal artery blood flow obtained from one subject on three separate occasions^a

| Occasion | D _s mm | θ degrees | V _{msa} cm·sec ⁻¹ | V _{sa} cm·sec ⁻¹ | Q̇ ml·min ⁻¹ |
|-----------|----------------------|--------------|--|---|----------------------------|
| 1 | R 3.1 | 70 | 81.4 ± 5.8 | 48.2 ± 2.4 | 275 ± 13 |
| | L 3.0 | 72 | 86.3 ± 3.2 | 46.6 ± 3.0 | 288 ± 15 |
| 2 | R 3.0 | 64 | 77.7 ± 7.3 | 44.4 ± 3.1 | 266 ± 14 |
| | L 3.0 | 68 | 81.1 ± 6.2 | 45.4 ± 7.2 | 292 ± 15 |
| 3 | R 3.1 | 63 | 76.4 ± 3.8 | 44.2 ± 2.4 | 256 ± 14 |
| | L 3.0 | 63 | 71.2 ± 4.9 | 42.6 ± 3.0 | 331 ± 24 |
| Mean ± SD | R 3.1 | 66 | 78.5 ± 2.6 | 45.6 ± 2.3 | 266 ± 10 |
| | L 3.0 | 68 | 79.5 ± 7.7 | 44.9 ± 2.0 | 304 ± 24 |

^a Subject was a 24-year-old female with a body surface area of 1.54 m².

which was graded as normal. Calculated D_s/BSA and Q/BSA values from the contralateral RRA were more than 1 SD below the values obtained for LRA. Due to the apparent increase in vascular impedance, the RRA was placed in grade 3. Subsequently, decreased right renal vasculature in the patient was indicated by (1) radionuclide scan evidence of an atrophic lower pole of the right kidney (right kidney size of 8.7 cm vs. left of 11.4 cm); (2) delayed uptake of radioopaque dye on the right side (approximately 200 msec); (3) elevated renal vein renins (ratio right to left, 2.4:1.0). These results are consistent with a grade 3 category.

Another angiographic correlate from a 64-year-old patient with renal failure is presented in Fig. 6. In the lower portion of this figure, the gain and reject setting have been adjusted to accentuate the vessel walls. The vessel walls and blood flow streamlines run anteriorly and then laterally giving a Doppler angle that is more acute than if one assumes the vessels run only in the transverse plane. The narrowed region at the RRA origin from the abdominal aorta gives a reduced value of D_s/BSA compared with control values. Additionally, there is an increased value of V_{msa}/BSA in the region of the stenotic lesion compared with the control value. Consequently, the vessel was correctly placed in grade 2. In the same patient, no lumen image or blood velocities were recorded in the LRA, and this vessel was placed in grade 4. But, the angiogram (upper portion) demonstrated a patent vessel with a hemodynamically significant lesion.

Table 4 presents a comparison of the noninvasive and angiographic grades obtained from all 18 examined vessels. There was qualitative agreement between angiographic evaluation and DS classification in 14 of the 16 vessels. Significantly, there was only one disagreement when grading a vessel as normal or abnormal. An angiographically normal vessel was noninvasively graded as having a mild proximal lesion. Normal renin levels supported the angiographic findings.

Discussion

Techniques using the ultrasonic Doppler velocimeter have been used successfully in the noninvasive evaluation of cardiac [6, 7] and peripheral arterial [8, 9] disease. Furthermore, recent reports have demonstrated the velocimeter can be used to estimate left ventricular stroke volume and cardiac output [16, 17]. These reports encouraged us to modify and to adapt the

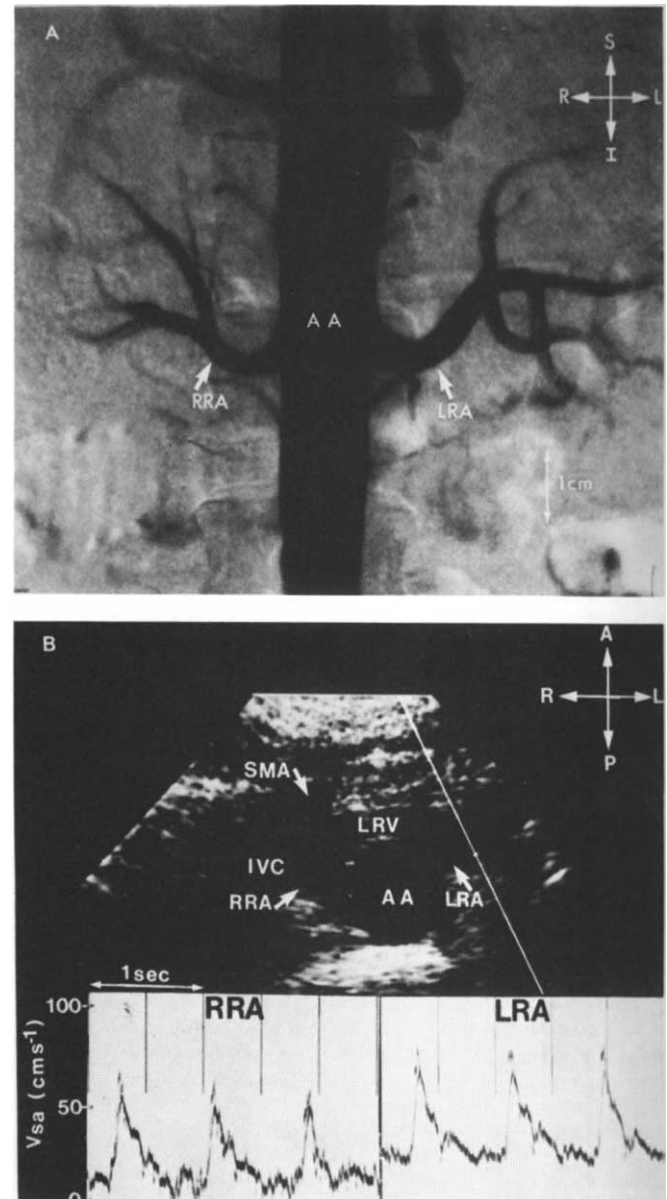


Fig. 5. **A** Anterior-posterior angiographic image of the right (RRA) and left (LRA) renal arteries obtained from a 33-year-old hypertensive patient with reduced renal artery vascularity on the right side suggested by independent methods. **B** Transverse gray-scale image and spatial average blood velocities (V_{sa}) obtained noninvasively from the LRA and RRA of the same patient. For demonstration purposes, instrument settings were adjusted in this image to allow identification of proximal anatomical landmarks. In a subsequent image, the settings were adjusted to delineate renal artery walls. Note the reduced V_{sa} in the RRA due to the suspected increase in vascular impedance. Other abbreviations are SMA, superior mesenteric artery; LRV, left renal vein; AA, abdominal aorta; IVC, inferior vena cava.

techniques with two-dimensional real-time Duplex scanning in the characterization of renal blood flow variables.

Sampson et al [18, 19] reported that it was feasible to monitor renal blood flow by continuous-wave Doppler ultrasound using a calibration according to the vessel diameter. This method elicited inaccurate results due to technical problems, such as the probe angle to the vessel, the probe distance from the

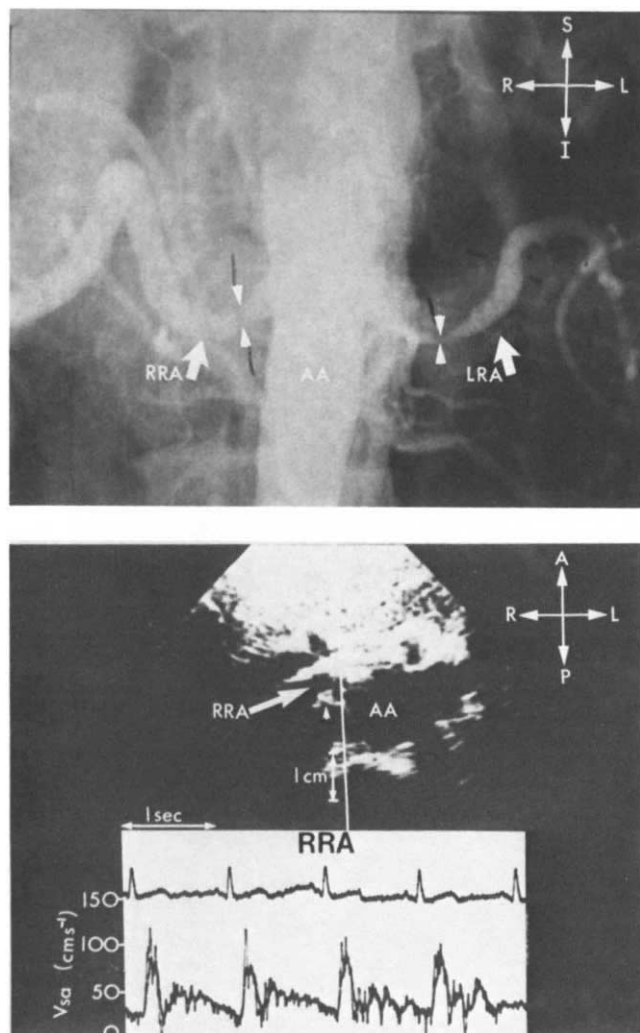


Fig. 6. **A** Angiographic image of the right (RRA) and left (LRA) renal arteries obtained from a patient with bilateral renal artery stenosis. **B** Transverse gray-scale image and spatial average blood velocity (V_{sa}) obtained noninvasively from the right renal artery (RRA) of the same patient. Note the increased value of V_{sa} ($\approx 100\text{-sec cm}^{-1}$) and the reduced lumen diameter in the RRA which runs anteriorly than laterally in the transverse section. No vessel image or flow velocity signal was obtained from the LRA. AA denotes the abdominal aorta.

vessel, and the contamination of the renal artery signal due to other adjacent arteries and veins. Arima et al [20] solved some of the aforementioned problems by utilizing a directional sensing ultrasonic Doppler flowmeter. The directional Doppler allowed separate recordings of arterial and venous blood velocities. Their analytical method was based on indirect timing indices. They concluded that use of the noninvasive Doppler ultrasonic velocimeter was a viable technique for evaluating the morphologic features and function of a renal graft. Although these techniques were able to provide valuable information about renal artery graft function, they were unable to provide quantitative information on normal and abnormal anatomy (lumen geometry) and physiology (blood flow variables).

The noninvasive characterization of renal blood flow requires the following four distinct steps: (1) location of the renal artery,

Table 4. Comparison of the angiographic and noninvasive Duplex scanner grading of 18 renal arteries.

| | Angiography | Noninvasive Duplex scanner |
|--------------------------------------|-------------|-------------------------------|
| Grade 1 Normal | 7 | 6 |
| Grade 2 Partial proximal obstruction | 7 | 8 |
| Grade 3 Increased vascular impedance | 2 | 1 |
| Grade 4 Proximal occlusion | 2 | 3 |
| Total | 18 | 18 |

(2) determination of the relative angle between the Doppler beam axis and the longitudinal axis of the renal artery, (3) measurement of the lumen area, and (4) measurement of the average velocity within the vessel. The first three problems apparently can be resolved by the dual frequency Duplex scanner with appropriate modifications [6–9]. Variable sample volume control [12, 13] and careful audio spectrum analysis [15] allow a more accurate measurement of average spatial velocity, which is multiplied by an independent measurement of lumen diameter (taken from the high resolution video display) to obtain flow rate. The dual frequency capability of this unit also allows maximum resolution consistent with adequate penetration.

As in all noninvasive ultrasonic methods, operator skill is of tantamount importance to obtain accurate and reproducible results. At times, procedures would require over 1 hour to obtain technically adequate studies. The influence of systematic and experimental errors must also be carefully considered and reduced [5, 10, 12]. Nevertheless, technically inadequate studies occurred in 21% of the initial normal group and 18% of the angiographically studied group even after repeated attempts. Improved transducer design with further operator experience may decrease these percentages.

The good correlation ($r = 0.98$) between \dot{Q}_T and \dot{Q}_{DS} in vitro strongly suggests that quantitative values of flow variables can be determined with the DS technique. Although the precision and accuracy of the calculation of \dot{Q}_{DS} was apparently independent of the value of θ (50° to 80°), which is arbitrarily selected during the in vitro calibration, the minimum angle should be used in vivo because the error of calculation of V_{sa} increases with the cosine function [5]. In vivo applications of the DS technique produced reproducible (Table 3) and physiologically reasonable (Tables 1 and 2) values [3]. Similar techniques have demonstrated good correlation with invasive flowmetry standards but in different anatomic locations [16, 17]. The statistically significant correlations ($P < 0.01$), between BSA with D_s and \dot{Q} help lend support to the validity of the DS technique. Although acoustic and anatomical scale factors may produce significant problems in relating correlates between simultaneous electromagnetic flowmeter and noninvasive DS measurements in the canine model to the human renal artery, these studies are presently being undertaken by this laboratory. Furthermore, a 20-MHz velocimeter-tipped catheter [21, 22] is presently being used to invasively measure renal artery blood velocities during elective renal angiography. Noninvasive DS measurements will be made simultaneously with the catheter-tipped velocity measurements to further determine the accuracy.

cy of the noninvasive technique and to monitor the response of the renal vasculature to the vasoactive influence of the radiographic contrast material.

In this blind study, the clinical utility of the DS technique was evaluated on 9 patients (18 renal arteries) subjected to renal angiography. Six of seven angiographically normal vessels were noninvasively graded as normal. The one exception was an angiographically normal vessel being graded as having a mild lesion. The DS categorization of the 13 angiographically documented abnormal renal vascular systems produced only one false-positive and no false-negative results. The only difference between the categorization of abnormal vessels by these two techniques occurred in a severely stenosed LRA that was incorrectly graded as totally occluded. This difference may be explained by the significantly diminished flow and extreme lumen reduction within this vessel.

Certainly this initial, nonrandomized clinical study will allow no definitive correlate to angiography (with its own limitations) to be made. Because the angiograms were made at two different centers during this preliminary study, high-quality subtraction images could not always be obtained (Fig. 6). Nevertheless, the available angiograms were clinically diagnostic, and the consistent agreement of the two techniques is encouraging. These results, although preliminary, indicate that an experienced operator can use a modified dual frequency DS system to effectively characterize blood flow variables in normal and diseased human renal arteries in a large portion (but not all) of the clinical population which could be helped by a noninvasive assessment of their renal vasculature.

We conclude that with careful technique the DS can be used to noninvasively characterize normal and abnormal renal artery blood flow variables in the human. Due to its noninvasive nature, the DS technique could be used to select appropriate candidates for invasive evaluation and to provide unique physiologic information. Furthermore, the DS can be used to evaluate patients whose clinical presentation does not warrant the use of costly and invasive modalities. The fact that this examination can be repeated on a frequent basis enhances the ability to obtain detailed studies of renal artery hemodynamics that are not hampered by constraints inherent in other methods.

Acknowledgments

I. Miranda, L. Fluit, M. Eldridge, G. Degenhart, and F. Pitman gave technical assistance; J. Davis, computer support; Dr. D. Erickson, patient referrals; and C. Thompson and D. Neff, secretarial assistance.

Reprint requests to Dr. E. R. Greene, Clinical Research Division, Lovelace Medical Foundation, 5400 Gibson Boulevard SE, Albuquerque, New Mexico 87108, USA

References

1. MAXWELL MH: Cooperative study of renovascular hypertension: Current status. *Kidney Int* 8(suppl):153, 1975
2. GENEST PB, KOIN E, KUCHEL O: *Hypertension*. New York, McGraw-Hill, 1977
3. BEESON PB, McDERMOTT W, WYNGAARDEN JB: *Textbook of Medicine*. Philadelphia, W. B. Saunders Company, 1979, pp 1210-1218
4. GOLDBERG BB: *Abdominal Gray Scale Ultrasonography*. New York, John Wiley and Sons, 1977.
5. BAKER DW, DAIGLE RE: Noninvasive ultrasonic flowmetry. in *Cardiovascular Flow Dynamics and Measurement*, edited by HWANG N, Houston, University Press, 1977, pp 151-189
6. BAKER DW: Applications of pulsed Doppler techniques. *Radiol Clinics N Am* 18:79-103, 1980
7. KALMANSON D, VERYROT C, ABITBOL G: Two-dimensional echo-Doppler velocimetry in mitral and tricuspid valve disease. in *Recent Advances in Ultrasound Diagnosis*, edited by KURJAK A. Amsterdam, Excerpta Medica, 1979, pp 335-348
8. PHILLIPS DJ, POWERS JE, EYER MK, BLACKSHEAR WM, BODILY KC, STRANDNESS DW, BAKER DW: Detection of peripheral vascular disease using the duplex scanner III. *Ultrasound Med Biol* 6:205-218, 1980
9. BLACKSHEAR WM, PHILLIPS DJ, CHIKOS PM, HARLEY JD, THIELE BL, STRANDNESS DE: Carotid artery velocity patterns in normal and stenotic vessels. *Stroke* 11:67-71, 1979
10. GREENE ER, HOEKENGA DE, RICHARD KL, DAVIS JG: Pulsed Doppler echocardiographic audio spectrum analysis: Time interval histogram versus multifilter spectrogram and fast Fourier transform. *Biomed Sci Instrum* 16:134-144, 1980
11. LUNT MH: Accuracy and limitations of the ultrasonic Doppler blood velocimeter and zero-crossing detector. *Ultrasound Med Biol* 2:1-10, 1975
12. GREENE ER, RICHARDS KL, NELSON C, DAVIS JG: Variable sample volume dimension in pulsed Doppler echocardiography. *Biomed Sci Instrum* 15:91-100, 1979
13. GREENE ER, RICHARDS KL, DAVIS JG: Improved sample volume control for pulsed Doppler echocardiography. *Circulation* 60(II):245, 1979
14. McDONALD DA: *Blood flow in arteries* (2nd ed). London, Edward Arnold Company, 1974
15. GILL RW: Pulsed Doppler with B-mode imaging for quantitative blood flow measurement. *Ultrasound Med Biol* 5:223-235, 1979
16. GREENE ER, LOEPKY JA, MATHEWS EC, HOEKENGA DE, RICHARDS KL, TUTTLE WC: Noninvasive Doppler stroke volume during rest and exercise. *Proc 33rd ACEMB* 22:23, 1980
17. DARSEE JR, WALTER PF, NAUTTER DE: Transcutaneous Doppler method of measuring cardiac output II. *Am J Cardiol* 46:613-618, 1980
18. SAMPSON D, ABRAMCZYK J, MURPHY FP: Ultrasonic measurement by bloodflow changes in canine renal allografts. *J Surg Res* 12:388, 1972
19. SAMPSON D: Ultrasonic method for determining rejection of human renal allotransplants. *Lancet* 2:976, 1979
20. ARIMA M, ISHIBASHI M, USAMI M, SAGAWA S, MIZUTANI S, SONODA T, ICHIKAWA S, IHARA H, NAGANO S: Analysis of the arterial blood flow patterns of normal and allografted kidneys by the directional ultrasonic Doppler technique. *J Urol* 122:587, 1978
21. COLE JS, HARTLEY CJ: The pulsed Doppler coronary artery catheter. Preliminary report of a new technique for measuring rapid changes in coronary artery flow velocity in man. *Circulation* 56:18-25, 1977
22. RICHARDS K, HARTLEY C, GREENE D: Usefulness of the Doppler Sones coronary and angiographic catheter. *Circulation* 62:111-99, 1980